Proceedings of the 2018
26th International Conference on Nuclear Engineering
ICONE26
July 22-26, 2018, London, England

ICONE26-82457

MEASURING EFFECTS OF RADIATION ON PRECIPITATES IN ALUMINUM 7075-T6 USING DIFFERENTIAL SCANNING CALORIMETRY

Rachel C. Connick
Mesoscale Nuclear Materials Laboratory
Laboratory for Nuclear Security and Policy
Department of Nuclear Science and Engineering
Massachusetts Institute of Technology
Boston, Massachusetts 02139
Email: rconnick@mit.edu

Charles A. Hirst
Penghui Cao
Kangpyo So
R. Scott Kemp
Michael P. Short*
Department of Nuclear Science and Engineering
Massachusetts Institute of Technology
Boston, Massachusetts, 02139
hereiam@mit.edu

ABSTRACT

Radiation damage in structural materials for nuclear applications is not well-understood, especially when linking the atomic scale damage mechanisms to the macroscopic effects. On a microscopic level, particle radiation creates defects that can accumulate in the material. Defects can also interact with existing features in the material. Since both defects and features have different energies associated with them, investigation of the resulting energy spectrum in a macroscopic sample may offer insight into the connection between microscopic damage and macroscopic properties.

In alloys, changes in the size and number of precipitates will be reflected in the amount of energy required to dissolve the precipitates during thermal analysis. This can then be studied using differential scanning calorimetry (DSC). This work explores the sensitivity of the DSC measurement to detect irradiation-induced instability in metastable and secondary phase precipitates in the high-strength aluminum alloy 7075-T6 for extremely low doses of helium-ion and neutron irradiation. The precipitates in aluminum 7075-T6 are expected to grow or shrink, changing the energy spectrum measured by DSC. The magnitude of the change can then be compared to a model of irradiation-induced phase instability. This will demonstrate the ability of this thermal analysis technique to help bridge the gap between microscopic radiation effects and macroscopic properties.

INTRODUCTION

Radiation material science is the study of how particle radiation degrades the material properties of structural metals. The mechanisms for radiation damage are studied from the initial interactions between the incident particles and the atoms in the irradiated material to how the microstructure in the material evolves after these interactions [1]. Different techniques are required to study different effects that occur over many orders of magnitude in both time and length scales, which make it impractical to study all effects at once. For example, the initial damage from the incident radiation occurs on atomic scales in nanoseconds. These scales are not generally observable with physical experiments and so are usually studied using atomic simulations. Computational costs, however, limit the number of atoms and length of time that can be simulated. This makes it challenging to predict and explain effects on, and evolution of, microstructural features because they require large size and time scales.

In the field of radiation material science, the standard unit of radiation damage or exposure is the dpa or displacements per atom. This is a calculated unit based on the conditions of irradiation as well as the material irradiated, using a ballistic model to predict an amount of damage in the material, and therefore

*Address all correspondence to this author.

requires a comprehensive knowledge and understanding of the system. Material properties measured using standard tests do not always correlate one-to-one with the dpa, depending on other conditions of an experiment. The development of physical techniques to measure and isolate effects of radiation on microstructural elements that are directly responsible for material performance could help to fill the gap in understanding between the initial radiation effects and resulting mechanical properties. One such technique utilizes differential scanning calorimetry (DSC), which measures thermal effects and enthalpies of reactions. In particular, the development of DSC to measure the effects of radiation in precipitate hardened metal alloys that have distinctive DSC signatures would therefore contribute to connecting the theories and simulations of radiation damage and the performance of engineering components.

Rather than predicting irradiated material properties, another alternative application of this DSC technique is in the forensic reconstruction of irradiation histories. For example, one could attempt verification of uranium centrifuge enrichment history (the most prominent technique for uranium enrichment as well as for states that attempt to acquire nuclear weapons [2]). The international community relies on producers records to verify the absence of highly enriched or weapons-grade uranium made in accordance with international treaties and agreements. It is theoretically possible, however, that a quantitative forensic technique could be developed to verify enriched uranium production history based on the radiation effects on the centrifuge wall caused by alpha particles emitted by the decay of the uranium in the centrifuge. One challenge, though, is that the irradiation rate experienced in a centrifuge application is about eight orders of magnitude less than that studied for nuclear reactor applications due to the low probability of radioactive decay in the uranium isotopes of interest. This work thus focuses on how to quantify the sensitivity of the DSC technique to such small amounts of radiation.

MATERIAL SELECTION

The material chosen for this study is the aluminum alloy 7075-T6. It is an Al-Mg-Zn alloy that is solution treated and precipitate hardened to the -T6 designated temper. In literature [3–6], the precipitate microstructural evolution is generally described as progressing from the supersaturated solid solution to homogeneously nucleated coherent Guinier-Preston (GP) zones to semi-coherent η' metastable precipitates to incoherent stable η phase precipitates, although more complex evolution has been described [4, 7]. While, thermodynamically, the equilibrium state of the material would contain only η phase precipitates, this would require unreasonably long amounts of aging time to achieve at the relatively low aging temperature. Thus, at the -T6 temper, all three types of precipitates may be present with η' being most prevalent, which is preferable due to the increased strength properties associated with small, finely dispersed precipitates [8].

RADIATION EFFECTS

Radiation in precipitate-hardened aluminum alloys has been observed to nucleate, dissolve, shrink, or grow precipitates, generally governed by the competing effects of ballistic mixing and diffusion [9]. The NHM model developed by Nelson, Hudson, and Mazey can be applied to a simplified aluminum 7075-T6 system, from which a critical precipitate size can be derived. Below this critical size, radiation will encourage precipitates to grow, and above this size, the precipitates will shrink [9–11]. In the NHM model of recoil dissolution, the growth rate of precipitates in a matrix during irradiation is determined by dissolution of the precipitate due to ballistic collisions knocking atoms out of the precipitate. However, because precipitation is thermodynamically favorable, diffusion of the solutes (Mg and Zn) from the matrix back to the precipitate can create an opposing effect. This is represented by the precipitate growth rate given by Equation 1, where D is the diffusivity of the solute in the matrix, C is the total concentration of the solute, C_{pr} is the concentration of the solute in the precipitate, ρ is the precipitate density, K_0 is the damage rate in dpa/s, and $\zeta\Omega$ represents the ballistic-driven flux of atoms away from the precipitate due to K_0. Nelson, Hudson, and Mazey estimate the $\zeta\Omega$ factor to be roughly 10^{-11} cm [10].

$$\frac{dr_p}{dt} = -\zeta\Omega K_0 + \frac{3DC}{4\pi r_p C_{pr}} - {r_p}^2 D\rho \tag{1}$$

To represent a simplified aluminum 7075-T6 system, some further assumptions will be made. The diffusivity of solute in the aluminum matrix will be taken to be 10^{-15} cm^2/s [11]. C and C_{pr} will be represented by 5% and 66% respectively, which are the concentrations of Zn in the alloy and η precipitates ($MgZn_2$). The precipitate density ρ will be estimated as 10^{15} per cm^3 [5]. Finally, the dpa rate can be estimated to be 10^{-15} dpa/s [11]. With these numbers, the critical precipitate radius occurs at a radius of 30 nm. It should be noted that this result is stable for a large range of dose rates. From literature characterizing aluminum 7075-T6, the size of precipitates can range from 10 to 100 nm, where η' precipitates tend to be less than 30 nm, while the η precipitates are larger [5]. Based on the NHM model of the simplified aluminum 7075-T6 system, this would then suggest that η' precipitates would grow while any η precipitates present would be inclined to shrink.

EXPERIMENTAL METHODS

The technique proposed to measure radiation effects is differential scanning calorimetry (DSC). Calorimetry is the mea-

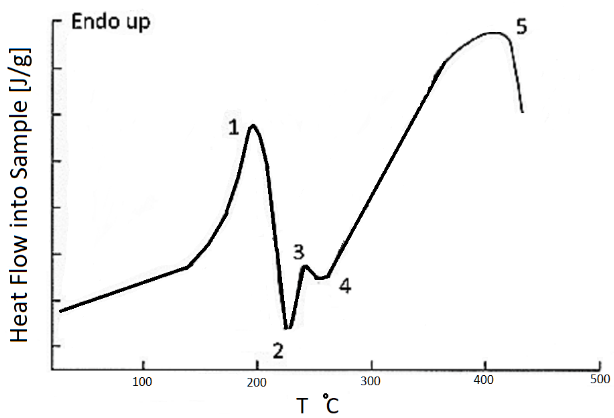

FIGURE 1. SCHEMATIC REPRESENTATION OF DSC SIGNAL BASED ON [6]. PEAKS AND TROUGHS ARE ATTRIBUTED TO DISSOLUTION AND FORMATION OF PRECIPITATES.

surement of energy released or absorbed in the form of heat during a process. In DSC, this measurement is conducted relative to a reference over a range of temperatures so that not only is the energy measured, but also the temperature dependency of the process is captured. For endothermic processes, more heat flow into the sample is required, while the opposite occurs for exothermic processes. What DSC produces, therefore, is an energy spectrum with peaks for endothermic processes and troughs for exothermic processes. Comparison of these peaks and troughs for irradiated and unirradiated samples could then reveal the effects of radiation on the microstructure of the aluminum 7075-T6.

DSC of aluminum 7075-T6 yields a very characteristic result, due to the temperature-dependent formation and dissolution of different types of precipitates over the course of heating [6]. A controversy around the interpretation of the result exists due to the complicated evolution of the precipitate microstructure [8, 12, 13]. An example of the characteristic spectrum is shown as a schematic in Figure 1. Using the simplified model for precipitation formation and evolution, Peak 1 is an endothermic peak which is usually associated with dissolution of GP zones. Exothermic Peak 2 (trough) represents the formation of η' precipitates, while Peak 3 is the endothermic dissolution of η'. Similarly, Peak 4 (trough) is the exothermic formation of η, and Peak 5 is the endothermic dissolution of η after it undergoes an Ostwald ripening process. The enthalpies of these reactions can be obtained by peak integration, which represents the energy released or absorbed during the reaction. Therefore, the peaks are also representative of how much of the phase underwent change. Thus, if radiation changes the amount of a phase present in precipitate form, the relative sizes of the peaks would also be expected to change. In the case of aluminum 7075-T6, the complexity of the precipitate evolution and microstructure and its corresponding DSC signal may offer an increased sensitivity to radiation effects due to the potential to detect effects by type of precipitate. Under the assumption that radiation will destabilize or stabilize different kinds of precipitates to varying magnitudes, a greater ability to distinguish between amounts and types of radiation can be achieved.

To test the effects of radiation of aluminum 7075-T6 at low doses, two sets of aluminum 7075-T6 samples were prepared for two kinds of irradiation experiments. The first set of experiments utilized helium-ion irradiation to create doses from 10^{-9} dpa to 10^{-6} dpa. The samples were prepared by cold rolling aluminum 7075 to a 30-micron foil (roughly 0.1 mg), before punching 4.5 mm diameter discs and heat treating. The T6 heat treatment consisted of solution treating the specimens at 450°C for 1 hour, quenching, and aging at 120°C for 24 hours. After this, four fluences of 3.4 MeV He^{2+} were used to reach 10^{-9}, 10^{-8}, 10^{-7}, and 10^{-6} dpa. For each fluence, three samples were irradiated. Three additional samples were set aside unirradiated to use as control samples. The total of fifteen samples were then subjected to DSC using a TA Instruments Discovery DSC with aluminum Tzero pans and lids. The heating protocol consisted of heating from 50°C to 550°C at 50°C/min with isothermal segments before and after at the starting and ending temperatures.

Because the range of 3.4 MeV helium ions is less than 30 microns in aluminum, the relative volume of damaged sample was limited to a fraction of the total sample volume. Thus, a second set of experiments was designed. Neutron irradiation was chosen due to its ability to create uniform damage in a much larger sample, which would produce a stronger signal in DSC. 10 mg samples with dimensions of approximately 2 x 3 x 0.7 mm were cut from aluminum 7075-T6 plate. Samples were then placed in the nuclear reactor at MIT (MITR) for a total of 1 hour of irradiation at a thermal flux of 5 x 10^{13} neutrons/cm^2 s (with a fast flux of 3 x 10^{12} neutrons/cm^2 s). This is equivalent to a dpa of about 10^{-5}, slightly higher than the upper range of the helium ion irradiations. Three samples were irradiated, and three were left unirradiated as controls. For each of these six samples, DSC was performed from 50°C to 550°C with a heating rate of 60°C/min.

RESULTS

All of the results exhibited the characteristic form expected of aluminum 7075-T6. Due to variations in the data obtained and the relatively small sample number of three, the analysis focuses on the peaks associated with the dissolution of GP zones and formation and dissolution of the η' precipitate. These appear as Peaks 1 and 2 in Figure 1. Peak integration provides a measure of the relative amounts of each phase. A demonstration of this analysis is shown in Figure 2. Peak 2 (a trough) was defined as the area between the signal and a horizontal line created from maximum signal of the adjacent peak. Peak 1 was then defined

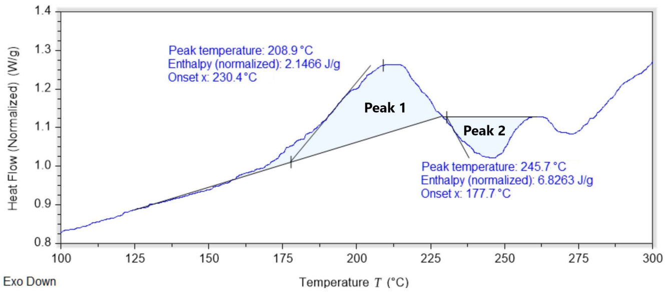

FIGURE 2. DATA ANALYSIS METHOD. SAMPLE WAS IRRADIATED WITH HELIUM IONS TO 1E-8 DPA. DSC WAS PERFORMED AT 50°C/MIN. PEAK 1 CORRESPONDS TO DISSOLUTION OF GP ZONES, WHILE PEAK 2 CORRESPONDS TO FORMATION OF THE η' PHASE.

as the area between the signal and a straight line connecting the left hand end of Peak 2 to the value of the signal at 125°C. Due to the arbitrary nature of the definitions of these baselines, the peak areas no longer can be said to accurately represent the enthalpies of the dissolution and formation events occurring. However, consistency in these definitions allows comparisons sample to sample.

For each fluence investigated, three samples were created and peak areas 1 and 2 integrated. The areas were recorded in units of J/g, and the like-fluence results were averaged. These results for both the helium and neutron irradiation experiments are shown in Figure 3. The error bars represent one standard deviation of each of the sets of three sample measurements. Based solely on the average values of the measurements as shown in Figure 3, radiation does cause a change in the peak areas measured. However, the size of the error bars throughout the results implies the differences in the measurements may not be statistically significant.

DISCUSSION

While the results shown in Figures 3A and 3B for helium irradiation do not show clear trends with increasing radiation dose, Figure 3B especially shows potential for establishing a sensitivity of this technique, or the smallest amount of radiation that causes a measurable change in the DSC signal peaks. Examining the first level of radiation exposure in Figure 3B compared to the unirradiated samples, there is an increase in peak area corresponding to increased formation of the η' phase. However, it should be noted that due to the definition of Peak 2 for this analysis, this apparent increase in peak area may also be due to an increase in the peak height of the adjacent endothermic peak corresponding to η' dissolution. These observations can be compared to the theory presented previously. Assuming some η phase precipitates existed before irradiation, the radiation would

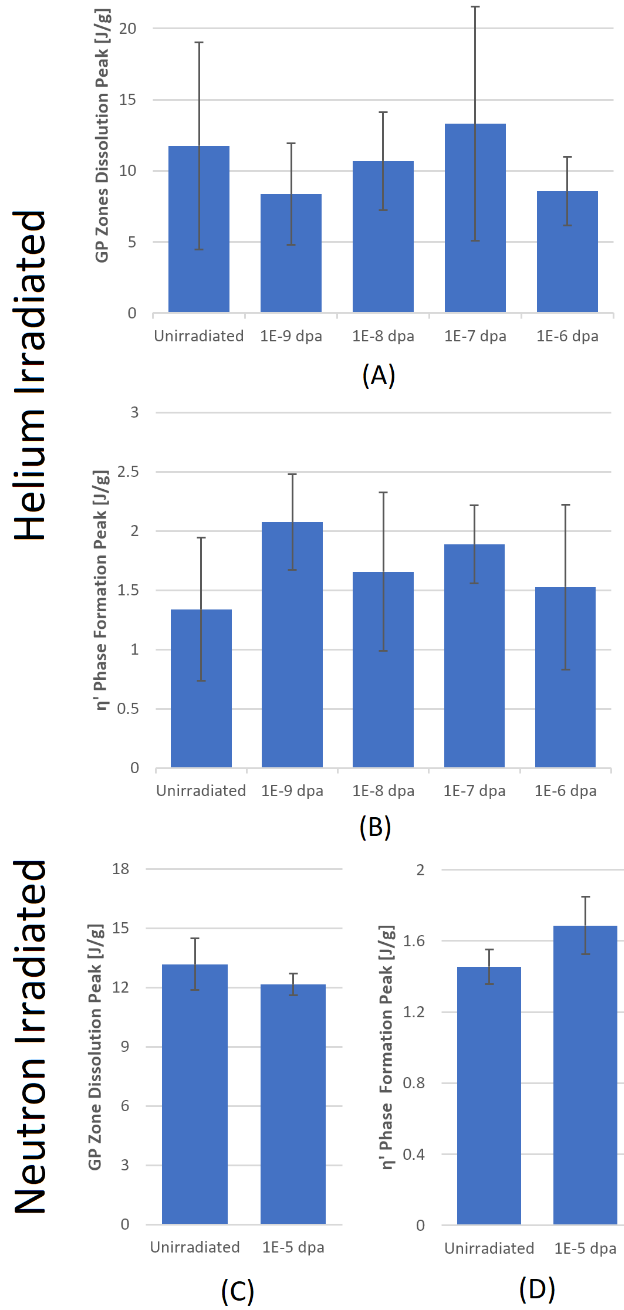

FIGURE 3. EXPERIMENTAL RESULTS. (A) GP ZONE DISSOLUTION PEAK AREAS FOR HELIUM IRRADIATED ALUMINUM 7075-T6 AT 4 DOSES COMPARED TO UNIRRADIATED CONTROL SAMPLE. (B) η' FORMATION PEAK AREAS FOR SAME SAMPLES AS (A). (C) GP ZONE DISSOLUTION PEAK AREAS FOR PRELIMINARY NEUTRON IRRADIATION EXPERIMENT COMPARED TO UNIRRADIATED CONTROLS. (D) η' FORMATION PEAK AREAS FOR SAME SAMPLES AS (C).

cause part of them to dissolve into the matrix. The dissolved solutes would then be available to diffuse to existing η' precipitates, which could result in more formation of the η' phase during the DSC experiment. Alternatively, small η precipitates might actually shrink to a small enough size that the strain on the crystal lattice due to the incoherency of the η phase could induce a transformation from η to η'.

The preliminary results of the neutron irradiation experiments are shown in Figures 3C and 3D. The magnitudes of the peak areas for the neutron irradiation experiments can be qualitatively compared with the unirradiated and highest exposure (1E-6 dpa) measurements from the helium-irradiation experiments in Figures 3A and 3B. First, for the GP zone dissolution peak areas, the unirradiated sample measurements match in magnitude fairly well, while the irradiated samples exhibit a decrease in peak area compared to the unirradiated samples (although the irradiated peak magnitudes do not match well). Secondly, for the η' formation peak areas, the independent irradiation experiments again exhibit the same trend of an increase in peak area between the unirradiated and irradiated measurements. Lastly, it should be noted that the relative sizes of the error bars are smaller for the neutron irradiation experiments, which is likely attributable to the greater mass of the neutron-irradiated samples producing a stronger DSC signal.

For all of the results in Figure 3, a key factor is the large deviations between measurements. It is thus likely that three samples per measurement is not enough to provide statistical confidence in the results. Assuming these experiments would fit a normal distribution, increasing the number of samples per measurement would likely reduce the standard deviations. This would provide more confidence in the sensitivity of the technique. However, if this method is to be used in forensic applications, some kind of correlation between amount of radiation and measured effects will have to be established. For this technique to be useful, confidence in the sensitivity of the measurement will not be enough. A comprehensive understanding of the effects of radiation on the precipitate microstructure must be achieved, which requires at least a more complete model of precipitate evolution.

CONCLUSION

The study of radiation effects on existing microstructural features such as precipitates facilitates the connection to models of radiation damage and therefore the radiation exposures. Based on the NHM model of disorder dissolution, aluminum 7075-T6 is expected to exhibit changes in its DSC signal after irradiation. Independent helium and neutron irradiation experiments do not disagree with this theory, and both exhibit similar results and trends. However, future work will focus on reducing the standard deviations in the measurements to improve confidence in the technique, as well as focusing on using a more complete model to base the theory on. With these improvements, a better quantitative analysis of the sensitivity of this DSC technique as a forensic tool will be achieved.

ACKNOWLEDGMENT

Thanks goes to K. Woller and CLASS for helium-ion irradiations, and the MIT Nuclear Reactor Laboratory for neutron irradiations. This work is supported in part by the Consortium for Verification Technology under Department of Energy National Nuclear Security Administration Award DE-NA0002534. This work is also supported in part by NSF Career Award #1654548.

REFERENCES

[1] Nordlund, K., Sand, A. E., Granberg, F., Zinkle, S. J., Stoller, R., Averback, R. S., Suzudo, T., Malerba, L., Banhart, F., Weber, W. J., Willaime, F., Dudarev, S., and Simeone, D., 2015. Primary radiation damage in materials. Tech. rep., OECD/NEA Working Party on Multiscale Modelling of Fuels and Structural Materials for Nuclear Systems, Expert Group on Primary Radiation Damage.

[2] Kemp, R. S., 2014. "The nonproliferation emperor has no clothes: The gas centrifuge, supply-side controls, and the future of nuclear proliferation". pp. 39–78.

[3] Viana, F., Pinto, A., Santos, H., and Lopes, A., 1999. "Retrogression and re-ageing of 7075 aluminium alloy: microstructural characterization". *Journal of Materials Processing Technology,* ***92-93***, pp. 54–59.

[4] Berg, L., Gjønnes, J., Hansen, V., Li, X., Knutson-Wedel, M., Waterloo, G., Schryvers, D., and Wallenberg, L., 2001. "Gp-zones in al-zn-mg alloys and their role in artificial aging". *Acta Materialia,* ***49***(17), pp. 3443 – 3451.

[5] Jacumasso, S. C., Martins, J. d. P., and Carvalho, A. L. M. d., 2016. "Analysis of precipitate density of an aluminium alloy by tem and afm". *REM - International Engineering Journal,* ***69***(4), pp. 451–457.

[6] Adler, P., Geschwind, G., De Iasi, R., and Dept, G. A. C. B. N. Y. R., 1971. *Calorimetric Study of Precipitation in a Commercial (7075) Aluminum Alloy*. Grumman Research Department memorandum. Defense Technical Information Center.

[7] Koch, S., and Antrekowitsch, H., 2007. "Study of the precipitation kinetics in almgzn alloys by using dsc".

[8] Park, J., and Ardell, A., 1989. "Correlation between microstructure and calorimetric behavior of aluminum alloy 7075 and al-zn-mg alloys in various tempers". *Materials Science and Engineering: A,* ***114***, pp. 197–203.

[9] Russell, K., 1984. "Phase stability under irradiation". *Progress in Materials Science,* ***28***(3-4), pp. 229–434.

[10] Nelson, R., Hudson, J., and Mazey, D., 1972. "The stability of precipitates in an irradiation environment". *Journal of Nuclear Materials,* ***44***(3), pp. 318–330.

[11] Was, G. S., 2007. *Fundamentals of radiation materials science*. Springer.
[12] Lloyd, D. J., and Chaturvedi, M. C., 1982. "A calorimetric study of aluminium alloy aa-7075". *Journal of Materials Science,* ***17***(6), Jun, pp. 1819–1824.
[13] Lendvai, J., 1996. "Precipitation and strengthening in aluminium alloys". *Materials Science Forum,* ***217-222***, pp. 43–56.